

Suppression of Higgs Mixing by Quantum Zeno Effect

Kodai Sakurai* and Wen Yin†

Department of Physics, Tohoku University, Sendai, Miyagi 980-8578, Japan

(Dated: April 6, 2022)

The Higgs portal interaction to a singlet sector of the standard model (SM) gauge group is widely-studied. In this Letter, we show that a quantum effect is important if the Higgs field mixes with another singlet scalar field whose decay rate is larger than the mass difference between the two mass eigenstates. This effect may be interpreted as the quantum Zeno effect. In either the quantum mechanics or the quantum field theory, we show that the resulting propagating mode is not the eigenstate of the mass matrix, but it is approximately the eigenstate of the interaction. As a consequence, the decoupling of the mixing effect happens at the infinity limit of the decay width of the exotic scalar even if the naïve mixing parameter is not small. With a finite decay width of the exotic scalar, we derive the effective mass of the propagating mode in the SM sector, its decay rate, and the couplings at the 1-loop level. It turns out that the mixed mass eigenstates can mimic the discovered 125 GeV Higgs boson. This fuzzy Higgs boson can be obtained in a simple perturbative renormalizable model. It is consistent with the 125 GeV SM Higgs boson when the mass difference is smaller than $O(0.1)\text{GeV}$ ($O(1)\text{GeV}$) for $O(1)$ ($O(0.01)$) mixing. We argue the possible natural scenario for the tiny mass splitting and the possibility that the upper bound of the mass difference is larger for a strongly-coupled singlet sector. To probe the fuzzy Higgs boson scenario, it is difficult to directly produce the singlet sector particles. Nevertheless, the future Higgs factories may probe this scenario by precisely measuring the Higgs boson invisible decay rate and the deviation of the Higgs coupling. Applications of the mechanism are also mentioned.

Introduction.— The existence of a gauge singlet sector, which we call the dark sector, is plausible due to the evidence of dark matter. In particular, the dark sector may include light particles since the stability is easily guaranteed for light dark matter. The dark sector may connect with the SM sector via a portal interaction between the Higgs and dark Higgs fields [1, 2].

In the broken phase, in general, the Higgs potential is given as, $V = \sum_{i=0} h^i V_{\text{dark}}^{(i)}$, with h being the Higgs boson that is embedded in the Higgs doublet field. $V_{\text{dark}}^{(i)}$ is the potential as a function of solely gauge-singlet fields and parameters. For concreteness, let us consider the renormalizable potential with $U(1)$ global and $U(1)_Y \times SU(2)_L \times SU(3)_c$ gauge symmetries:

$$V = -m_\Phi^2 |\Phi|^2 + \lambda |\Phi|^4 + \lambda_P |H|^2 |\Phi|^2 + \lambda_H |H|^4 - \mu_H^2 |H|^2. \quad (1)$$

Here Φ (H) is the dark (SM) Higgs field, which is gauge singlet (doublet), whose vacuum expectation value (VEV) will break the $U(1)$ ($SU(2)_L \times U(1)_Y$) symmetry; $\lambda_P, \lambda(>0)$ and $\lambda_H(>0)$ are coupling constants; μ_H^2 and m_Φ^2 are the bare mass parameters. A slight modification of the model has been studied in the context of axion/dark photon dark matter production via the phase transition [3], the UV model of a CP-even ALP [4], WIMP [5–7][8–12], electroweak baryogenesis [5, 13] and collider physics [4, 10, 12, 14, 15].

The symmetry breaking occurs because of $\langle \Phi \rangle = v_s, \langle H_0 \rangle = v$. We obtain a massless Nambu-Goldstone boson (NGB), a , from the $U(1)$ breaking. This model is

not very special for realizing the mechanism in this Letter. The general and important feature is that we can define the “flavor”, similar to the neutrino oscillation, by the (broken) gauge symmetry, i.e. h is the SM flavor, and the other, s , is the dark flavor:

$$H = \left(\frac{G^+}{\frac{1}{\sqrt{2}}(v + h + iG^0)} \right), \quad \Phi = \frac{1}{\sqrt{2}}(v_s + s + ia), \quad (2)$$

where G^+ and G^0 are NGBs absorbed by the longitudinal mode of the weak gauge bosons. In general, s and h are not mass eigenstates since they mix with each other.

When the mixing is relatively small, s is almost the mass eigenstate ϕ_2 with the mass m_2 . Thus s can dominantly decay into a pair of the NGBs, a . The decay rate is $\Gamma_s[m_2] \equiv \frac{m_2^3}{32\pi v_s^2} \simeq \frac{\lambda_s m_2}{8\pi}$. When $\lambda_s = \mathcal{O}(1) - 4\pi$, the upper of which is a perturbative unitarity bound, $\Gamma_s = \mathcal{O}(10\% - 1)m_2$. Therefore, there is a parameter region

$$|m_2 - m_1| \lesssim \Gamma_s \lesssim m_2, \quad (3)$$

when $|m_2 - m_1| \lesssim \mathcal{O}(10\% - 1)m_2$ is satisfied. Here m_1 is the mass of the other mass eigenstate ϕ_1 . The region satisfying (3) is our focus. A relativistic state with momentum p has the decay time $t_s \sim p/(m_2 \Gamma_s)$ which is shorter than the timescale of $t_{\text{unc}} \sim 2p/(|m_2^2 - m_1^2|) \sim p/(m_2 |m_2 - m_1|)$ for measuring the energy difference according to the uncertainty principle. Therefore, the timescale that defines the mass eigenstates as the asymptotic states e.g. [16] does not exist.

To study the system with (3), for clarity, we consider the following Higgs production process in an electron-positron collider:

$$e^+ e^- \rightarrow Zh (= \cos \alpha \phi_1 - \sin \alpha \phi_2). \quad (4)$$

* kodai.sakurai.e3@tohoku.ac.jp

† yin.wen.b3@tohoku.ac.jp

We emphasize that h is the SM flavor eigenstate, which is a superposition of the mass eigenstates, ϕ_1 and ϕ_2 . α is the mixing angle.

In this Letter, we show that a quantum effect is so important that the on-shell state is *NOT* the mass eigenstate ϕ_i . This may be interpreted as the quantum Zeno effect e.g. [17] by defining the decay of s as the measurement. It states that the quantum system with frequent measurements evolves in a subspace of the total Hilbert space. The frequent decay of the dark flavor state forces the SM flavor state to evolve within itself, i.e. the Higgs mixing interactions with the dark Higgs boson are decoupled. To distinguish from the conventional SM Higgs boson, we call the propagating SM flavor state, fuzzy Higgs boson. We derive the property of the fuzzy Higgs boson: the mass, the decay rate, and the couplings, and show that it can be consistent with the SM Higgs boson, and thus the discovered Higgs boson with the mass of 125 GeV might be the fuzzy one. It is key to probe this scenario by precisely measuring the Higgs boson property.

Let us list some relevant studies. In the context of the physics beyond the SM (BSM), the quantum effect leading to the invalid use of naïve asymptotic state was studied widely (Within the SM plus neutrino masses, the neutrino oscillation and meson oscillation phenomena belong to this category.) For instance, there are baryogenesis mechanisms via right-handed neutrino oscillations [18–20] and via the left-handed neutrino oscillations [21–23] (see also quark flavor oscillations [24] and hadron oscillations [25–27]). Oscillation effects of axions [28] or gauge bosons [29] motivated by extra-dimensional models are also interesting. In [29, 30], it was pointed out that appropriate treatment of the Breit-Wigner formulation [31] is necessary in case the mass difference between two heavy scalar (vector) bosons is close to their widths. In [30, 32–38], the phenomenological implications of the interference effects of multiple nearly-mass degenerate scalar particles with same gauge charges, e.g. Higgs doublets and sleptons, are studied. In [10], applying the Breit-Wigner formulation, a similar model to our setup was investigated with MeV decay width of s but the region of our interest was not the authors' focus. What is new in our setup is that the dark flavor state has a large decay width. As far as we know, the suppression of the Higgs mixing effect by the large width has not been clearly pointed out and the resulting fuzzy Higgs property has not been well studied.

It was noticed that the nearly degenerate two Higgs bosons are favored to have consistent cosmology and low-energy phenomenology [12, 13]. In particular, the current LHC does not have enough detector resolution to constrain the decays of the degenerate Higgs bosons into the SM particles whose widths together are similar to that of the SM Higgs boson [39]. In contrast, by omitting the quantum Zeno effect, this is not true in our setup, because the two mass eigenstate bosons would decay invisibly due to the mixing. Thus both the SM interaction and the invisible decay branching fraction would be con-

strained. We will discuss that the constraints can be alleviated by increasing the decay width of the dark flavor scalar.

Intuitive discussion from quantum mechanics.—

Let us first discuss the system in an intuitive way by using quantum mechanics to relate the quantum Zeno effect. The reader, who would like to have rigid discussions, should move to the next part.

We define the SM flavor state as $|h\rangle$, which only couples to the SM particles, and the dark flavor state as $|s\rangle$, who only couples to the dark sector particles at the vanishing limit of λ_P . The mass eigenstates are defined as $|i\rangle$ with $i = 1, 2$. Then the mixing parameter is defined to satisfy $\cos \alpha \equiv \langle 1|h\rangle$, $\sin \alpha \equiv \langle 2|h\rangle$, $\langle 1|s\rangle = -\sin \alpha$, $\langle 2|s\rangle = \cos \alpha$.

Now we can follow the time evolution of $|h\rangle$ with the relativistic momentum \vec{p} at the time $t = 0$. We obtain the probability to measure $|s\rangle$ flavor state at the time t as

$$P[t] = \left| \langle s, \vec{p} | \exp[-i\hat{H}_{\text{free}}t] | h, \vec{p} \rangle \right|^2 \approx 4 \cos^2 \alpha \sin^2 \alpha \sin^2 \left(\frac{\epsilon}{4|\vec{p}|} t \right) \quad \text{with } \epsilon \equiv m_1^2 - m_2^2 \quad (5)$$

where \hat{H}_{free} is the free Hamiltonian, which defines the mass eigenstates of $|1\rangle$ and $|2\rangle$. The eigenvalues are $\sqrt{\vec{p}^2 + m_1^2}$, and $\sqrt{\vec{p}^2 + m_2^2}$, respectively. In the last equality, we have expanded m_i . We note that the quantum mechanics treatment is only valid at a short enough timescale. When t is longer than the life-time of s , $t_s \sim |\vec{p}|/(\bar{m}_s \Gamma_s[\bar{m}_s])$, we have to take account of the s decay. Here \bar{m}_s is the effective mass of the dark flavor and it is a certain average of m_i . If we define the decay as the measurement of $|s\rangle$, we may consider that the measurements take place in the period of $\sim t_s$. The measurement $|s\rangle$ with the probability of

$$P[t_s] \approx 4 \cos^2 \alpha \sin^2 \alpha \left(\frac{\epsilon}{4\bar{m}_s \Gamma_s[\bar{m}_s]} \right)^2. \quad (6)$$

Here we have used that $t_s \lesssim |\vec{p}|/|\epsilon|$. h also decays into the SM particles in reality, but we neglect it for illustrative purposes (This is included in the following numerical estimation.)

At $t = t_s$, the SM flavor is measured with the probability $1 - P[t_s]$. Later, the quantum state starts to evolve again from $|h\rangle$. In every t_s step this measurement happens. Therefore at $t \gg t_s$ we can measure the SM flavor with the probability

$$P_h[t(\gg t_s)] \sim (1 - P[t_s])^{\frac{t}{t_s}} \sim \exp[-P[t_s] \frac{t}{t_s}]. \quad (7)$$

If $t \ll t_s/P[t_s]$, i.e. the measurement of $|s\rangle$ is too frequent, one finds $|h\rangle$ at any time of its propagation. This can be interpreted as the quantum Zeno effect due to the multiple frequent “measurements” via the $|s\rangle$ decay.

The energy of $|h\rangle$ is obtained as $\bar{E}_h \simeq \langle h, \vec{p} | \hat{H}_{\text{free}} | h, \vec{p} \rangle \simeq |\vec{p}| + \frac{m_1^2 \cos^2 \alpha + m_2^2 \sin^2 \alpha}{2|\vec{p}|}$. Thus we get the effective mass of the propagating state, $m_{\text{heff}}^2 \equiv \bar{E}_h^2 - \vec{p}^2$, as

$$m_{\text{heff}} \simeq \sqrt{m_1^2 \cos^2 \alpha + m_2^2 \sin^2 \alpha}. \quad (8)$$

From Eq. (7) we find that the SM flavor eigenstate has a decay rate of

$$\Gamma_{h \rightarrow \text{dark}} \sim \frac{p}{m_{\text{heff}}} \frac{P[t_s]}{t_s}. \quad (9)$$

On the contrary, in the conventional perturbation theory, the invisible decay rate of the Higgs flavor is estimated as $\frac{(|\langle s|1\rangle\langle 1|h\rangle|^2 + |\langle s|2\rangle\langle 2|h\rangle|^2)}{t_s} \sim 2 \cos^2 \alpha \sin^2 \alpha / t_s$ with $m_1 \sim m_2$. Our result gives a further suppression by $\sim \left(\frac{\epsilon}{4\bar{m}_s \Gamma_s [\bar{m}_s]} \right)^2$. In the following, we will confirm this intuitive discussion by quantum field theory.

Breit-Wigner formulation.— To study the propagating mode, we can estimate the full two-point function. To this end, we estimate the resummed propagator. The propagator in the flavor basis is

$$\hat{\Delta} = iR \cdot \begin{pmatrix} Q^2 - m_1^2 + \hat{\Pi}_{11} & \hat{\Pi}_{12} \\ \hat{\Pi}_{21} & Q^2 - m_2^2 + \hat{\Pi}_{22} \end{pmatrix}^{-1} \cdot R^T. \quad (10)$$

Here $\hat{\Pi}$ is the renormalized self-energy in the mass basis, and $R_{h1} \equiv \langle h|1\rangle = \cos \alpha$, $R_{h2} \equiv \langle h|2\rangle = -\sin \alpha$ and so on. We perform the 1-loop calculation of the self-energy to obtain

$$\hat{\Pi}_{ij} \simeq \frac{i}{32\pi v_s^2} \begin{pmatrix} \sin^2(\alpha) m_1^4 & \sin \alpha \cos \alpha m_1^2 m_2^2 \\ \sin \alpha \cos \alpha m_1^2 m_2^2 & \cos^2(\alpha) m_2^4 \end{pmatrix} \quad (11)$$

where we used the on-shell renormalization (c.f. [40, 41]), and thus the real part is dropped by the renormalization conditions. Here we omit to write down the subdominant contribution of the imaginary part from the Higgs decay into the SM particles for clarity. The full 1-loop formulas are given in Appendix A.

According to the LSZ reduction or optical theorem, the mass of the particle corresponds to the real part of the pole of the resummed propagator, and the decay rate of the propagating mode can be obtained from the imaginary part. Since we are interested in $|\epsilon| = |m_1^2 - m_2^2| \ll \Gamma_s m_{\text{heff}} \sim \frac{m_{\text{heff}}^4}{32\pi v_s^2}$, we expand the denominator, $\det[(-i\hat{\Delta})]^{-1}$, of the propagator with ϵ . By noting $m_1^2 = m_{\text{heff}}^2 + \epsilon \cos^2 \alpha$, $m_2^2 = m_{\text{heff}}^2 - \epsilon \sin^2 \alpha$, the denominator factorizes as

$$\begin{aligned} \text{denominator of } \hat{\Delta} &\simeq (Q^2 - m_{\text{heff}}^2 + \epsilon \cos(2\alpha) + i \frac{m_{\text{heff}}^4}{32\pi v_s^2}) \\ &\times (Q^2 - m_{\text{heff}}^2 + \frac{\epsilon^2 \sin^2(2\alpha)}{2m_{\text{heff}}^2} + i \frac{8\pi \epsilon^2 \sin^2(2\alpha) v_s^2}{m_{\text{heff}}^4}). \end{aligned} \quad (13)$$

Here we have neglected higher-order terms in ϵ that are irrelevant for analytic estimation. This is common in any component of $\hat{\Delta}_{\beta\gamma}$ ($\beta, \gamma = h, s$). The real parts of the two poles are separated by $\mathcal{O}(\epsilon)$, which is smaller than the imaginary part of Eq. (12), $\frac{m_{\text{heff}}^4}{32\pi v_s^2} \simeq \Gamma_s m_{\text{heff}}$. We can also find

$$\text{numerator of } \hat{\Delta}_{hh} \simeq i(Q^2 - m_{\text{heff}}^2 + \epsilon \cos(2\alpha) + i \frac{m_{\text{heff}}^4}{32\pi v_s^2}) \quad (14)$$

which is the same as (12) at the leading order of ϵ in either real and imaginary part. As a consequence, we obtain

$$\hat{\Delta}_{hh} \simeq \frac{i(1 + \delta)}{Q^2 - m_{\text{heff}}^2 + \frac{\epsilon^2 \sin^2(2\alpha)}{2m_{\text{heff}}^2} + i \frac{8\pi \epsilon^2 \sin^2(2\alpha) v_s^2}{m_{\text{heff}}^4}}. \quad (15)$$

Here δ denotes the higher order correction of order ϵ^2 . For instance, we obtain $\delta(Q^2 \simeq m_{\text{heff}}^2) \simeq -\sin^2(2\alpha) \frac{\epsilon^2 (m_{\text{heff}}^2 + 32i\pi v_s^2)^2}{4m_{\text{heff}}^8}$ around the pole while it is further suppressed by $Q^2 - m_{\text{heff}}^2$ far away from the pole.

Interestingly $\hat{\Delta}_{hh}$ behaves as a propagator with a single pole. From the real part, we obtain that the mass of the propagating mode to be m_{heff}^2 with a tiny correction of $\mathcal{O}(\epsilon^2/m_{\text{heff}}^2)$ consistent with Eq. (8). The decay rate into the dark sector is read from the imaginary part,

$$\Gamma_{\text{heff} \rightarrow \text{dark}} \simeq \frac{\epsilon^2 \sin^2(2\alpha)^2}{4m_{\text{heff}}^2 \Gamma_s [m_{\text{heff}}]} \quad (16)$$

which is consistent with Eq. (9). $|\hat{\Delta}_{sh,hs}(Q^2 \sim m_{\text{heff}}^2)| \simeq \left| \frac{\epsilon \sin(2\alpha)}{2m_{\text{heff}} \Gamma_s [m_{\text{heff}}]} \frac{i}{Q^2 - m_{\text{heff}}^2} \right|$ around the pole. $\hat{\Delta}_{ss}$ includes the two poles. The numerator of $\hat{\Delta}_{hh}$ and $\hat{\Delta}_{hs}$ at around the pole is similar to the system that the Higgs mixes with a (decoupled) heavy particle decaying into the dark particles c.f. [4] by defining the effective mixing angle

$$\sin[2\alpha_{\text{eff}}] \simeq \frac{\epsilon \sin(2\alpha)}{m_{\text{heff}} \Gamma_s [m_{\text{heff}}]}, \quad (17)$$

by noting that the numerator of $\hat{\Delta}_{hs}$ ($\hat{\Delta}_{hh}$) around the pole is $\sin \alpha_{\text{eff}} \cos \alpha_{\text{eff}}$ ($\cos^2[\alpha_{\text{eff}}]$) at the leading order. This expresses that the fuzzy Higgs boson coupling to the SM particles is $g_{\text{heff}XX}^{\text{SM}} = g_{hXX}^{\text{SM}} \cos[\alpha_{\text{eff}}]$. Here g_{hXX}^{SM} is the tree-level Higgs boson coupling within the SM.

Fuzzy Higgs boson as the 125 GeV one.— Including full 1-loop corrections, we plot $|\hat{\Delta}_{hh}|$ in Fig.1 by varying Q for $\alpha = \pi/4, \epsilon = 25 \text{ GeV}^2$ and $\alpha = 0.01, \epsilon = -1600 \text{ GeV}^2$ in the top and bottom panels, respectively, in colored solid lines. In the top (bottom) figure, we fix $m_{\text{heff}} = 125.25 \text{ GeV}$ with $v_s = 1000, 500, 100$, and 30 GeV ($10^4, 10^3, 100$, and 30 GeV). Decreasing v_s corresponds to the increase of Γ_s . One can see that the two peaks at large v_s become a single one by decreasing v_s , while the single peak position approaches

to m_{heff} . We also denote the usual SM Higgs propagator by the black dashed line. When v_s gets smaller, $\hat{\Delta}_{hh}$ approaches to the SM Higgs one.

Also shown in the built-in panels are the peculiar features of the fuzzy Higgs decay width into aa . This is estimated from the width of the propagator involving only a loops. The colored points correspond to the same colored lines for $|\hat{\Delta}_{hh}|$. The horizontal blue-dashed line corresponds to the current constraint of the branching fraction by ATLAS, 11% [42] (see also Refs. [43, 44]). Thus the invisible decay can be consistent with the observation with sufficiently small v_s .

In the region satisfying the invisible decay bound in the two figures, the size of effective mixing $\sin[\alpha_{\text{eff}}]^2 \cos[\alpha_{\text{eff}}]^2 \simeq \Gamma_{\text{heff} \rightarrow \text{dark}} / \Gamma_s[m_{\text{heff}}] \lesssim \text{MeV} / \Gamma_s[m_{\text{heff}}]$ is tiny and the deviations of the couplings are very small (c.f. [45, 46]). There are also other loop corrections, rather than the imaginary part contribution, to the fuzzy Higgs coupling but they are even smaller (see Appendix B). Thus the discovered Higgs boson can be consistent with the fuzzy Higgs boson who is the superposition of the mass eigenstates.

Since it is difficult to produce a resonance absent in $\hat{\Delta}_{hs}$ or $\hat{\Delta}_{hh}$ in a SM particle collider, detecting the light s may not be easy.¹ One way to probe this scenario may be the Higgs invisible decay. Therefore probing this scenario is favored in the future lepton colliders such as FCC-ee, CEPC, ILC, CLIC [47–50].² When the mass difference is smaller or around MeV, Γ_s does not need to be much larger than $\mathcal{O}(\text{MeV})$. In this case, the effective mixing can get larger, and the fuzzy Higgs boson can be also probed by precisely measuring its couplings.

So far, for concreteness, the mechanism is explained by using a simple elementary particle model that is perturbative. The perturbative unitarity gives a lower limit $v_s \gtrsim 25 \text{ GeV}$ with the criterion $|a_0^i| < 1$ for the eigenvalues a_0^i of scattering matrix for the scalar bosons [51]. Since the red points corresponding to $v_s = 30 \text{ GeV}$ are close to the experimental bounds in Fig. 1, the fuzzy Higgs parameter region has the mass difference smaller than $|\epsilon|/m_{\text{heff}} = \mathcal{O}(0.1) \text{ GeV}$, and $\mathcal{O}(1) \text{ GeV}$ for $\alpha = \mathcal{O}(1)$ and $\mathcal{O}(0.01)$ respectively.

Application to other dark sectors.— An example of a natural perturbative model for the fuzzy Higgs boson can be obtained with a mirror SM, i.e. a dark sector that the SM transforms into via an exact Z_2 mirror symmetry. In this case, the dark Higgs decay width is around $\sim 4 \text{ MeV}$ and the mixing is $\alpha = \pi/4$ by introducing a small portal coupling, λ_P . The splitting of the two Higgs boson eigenmasses gets smaller with smaller $|\lambda_P|$. To evade the invisible decay bound, $\sin(\alpha_{\text{eff}}) \lesssim 0.2$. Thus, the

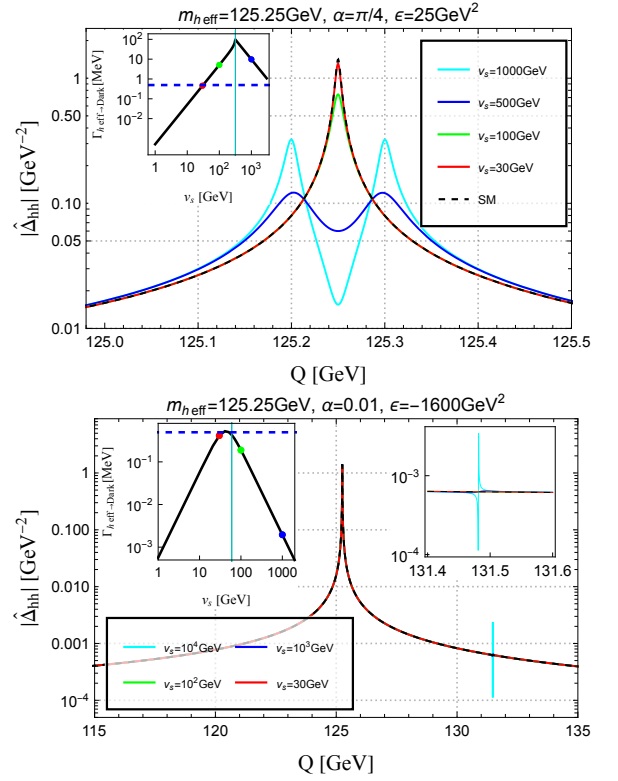


Figure 1. The (h,h) element of the resummed propagator, $|\hat{\Delta}_{hh}|$, by varying Q^2 . In the top (bottom) panel, we fix $\alpha = \pi/4$ (0.01), $m_{\text{heff}} = 125.25 \text{ GeV}$, $\epsilon = 25 \text{ GeV}^2$ (-1600 GeV^2) and plot the case $v_s = 10^3, 500, 100, 30 \text{ GeV}$ ($10^4, 10^3, 100, 30 \text{ GeV}$) in cyan, blue, green, red solid lines, respectively. These inputs yield $m_1 = 125.3 \text{ GeV}$ (125.25 GeV) and $m_2 = 125.2 \text{ GeV}$ (131.5 GeV) in the top (bottom) panel. Also shown is the resummed pure SM Higgs propagator in the black dashed line. The corresponding decay widths of the fuzzy Higgs boson are shown in built-in figures with the horizontal blue dashed line being the current bound. The colored points correspond to the same colored lines for $|\hat{\Delta}_{hh}|$. The vertical cyan line in each figure denotes $\Gamma_s[m_{\text{heff}}] \approx |m_1 - m_2|$ for comparison.

mirror SM can be probed via the invisible decay and the coupling measurement of the fuzzy Higgs boson.

We expect, on the other hand, that the upper bound of the mass difference can be relaxed if s connects a strongly-coupled dark sector e.g. by considering that dark sector particles are composite. Then the perturbative unitarity is not needed. Even if the dark sector is strongly coupled, the SM perturbativity should be under control since all the radiative contributions to the SM sector are suppressed if the portal coupling is small (see c.f. Appendix B).

Applications to cosmology.— In various cosmological scenarios, like baryogenesis, mediator, and light dark matter, one may have interesting parameter regions with the quantum Zeno effect in the vacuum. In the early Universe, however, the quantum Zeno effect may be ineffective due to the larger thermal/effective mass differences.

¹ That said, s may be produced via the $h_{\text{eff}}ss$ or $h_{\text{eff}}h_{\text{eff}}ss$ vertex from the portal coupling. But this cross-section is small due to the small $|\lambda_P|$ (Note that we have either small ϵ or α).

² Giving mass to a may induce the a decay into the SM particles, which give interesting other signatures [4].

The discussion in this Letter can be easily extended to other models with multiple particles. For instance, there are models describing the early Universe cosmology with many axions with one of them having a large decay rate/dissipation rate for reheating e.g. [52, 53]. In this case, the quantum Zeno effect may be important. Alternatively, a similar effect may explain the stability of the dark matter. For instance, we can consider two mass eigenstate axions, a_1 , and a_2 , both decaying into photons via the couplings $(\cos\beta a_1 + \sin\beta a_2)g_{a\gamma\gamma}F\tilde{F}$ with F (\tilde{F} , $g_{a\gamma\gamma}$) being the photon field strength (its dual, photon coupling) and β being the mixing angle. If the mass difference is much smaller than the decay rate, then $A \equiv (-\sin\beta a_1 + \cos\beta a_2)$, which is not the mass eigenstate of the Lagrangian parameter, behaves as the propagating mode. In addition, it is stabilized in the case the mass is close. Thus A can become long-lived dark matter. Axion mass difference may depend on temperature such that the axions both decay in the early Universe. This time-dependent decay effect may provide a production mechanism of the axion abundance similar to that in the ALP miracle scenarios [52, 54] (see also [55–59]).

Conclusions.— The Higgs portal interaction to a dark sector of the standard model gauge group is widely studied. In this Letter, we have shown that a quantum effect is important if the Higgs field mixes with another singlet scalar field whose decay rate is larger than the mass difference between the two mass eigenstates. The resulting propagating mode is approximately the eigenstate of the interaction, and it is different from the eigenstates of the mass matrix. As a consequence, the mixing interaction is suppressed with a sufficiently large decay width of the exotic scalar even if the naïve mixing parameter is not small. From the derived property, it turned out that the mixed mass eigenstates can mimic the discovered 125 GeV Higgs boson, giving a possibility that it is a single fuzzy Higgs boson. The future Higgs factories are important to reveal whether the 125 GeV Higgs boson is a fuzzy one by precisely measuring the Higgs boson invisible decay rate and the deviation of the Higgs coupling. The mechanism also has various applications.

Acknowledgement.— We thank Gi-Chol Cho, Yuki-nari Sumino and Masahiro Hotta for useful discussions. This work was supported by JSPS KAKENHI Grant Nos. 20H01894 (K.S.) 20H05851 (W.Y.), 21K20363 (K.S.), 21K20364 (W.Y.), 22K14029 (W.Y.), and 22H01215 (W.Y.).

Appendix A: Analytical formulae of the self-energy for Higgs bosons

The analytical expressions for the self energies Π_{ij} ($i, j = 1, 2$) with full 1-loop corrections in the mass basis are presented. In the calculation of Π_{ij} , We choose the 't Hooft-Feynman gauge. They are given in terms of the Passarino-Veltman functions [60]. We first separate Π_{ij} to each loop contribution as

$$\Pi_{ij} = \sum_f \Pi_{ij}^f + \Pi_{ij}^V + \Pi_{ij}^{\text{PT}} + \Pi_{ij}^S + \Pi_{ij}^a. \quad (\text{A1})$$

Each ingredient is given by

$$(16\pi^2)\Pi_{ij}^f = -R_{hi}R_{hj} \frac{4N_f^c m_f^2}{v^2} \left\{ A(m_f) + \left(2m_f^2 - \frac{Q^2}{2} \right) B_0(Q^2, m_f, m_f) \right\}, \quad (\text{A2})$$

$$\begin{aligned} (16\pi^2)\Pi_{ij}^V &= \frac{1}{2}g^2 R_{hi}R_{hj} \left(\frac{8}{\delta_{ij}+1} - 1 \right) A(m_W) \\ &+ \frac{1}{4}g_Z^2 R_{hi}R_{hj} \left(\frac{8}{\delta_{ij}+1} - 1 \right) A(m_Z) \\ &- \frac{1}{2}g^2 R_{hi}R_{hj} \left(\frac{1}{\delta_{ij}+1} + 1 \right) 4m_W^2 \\ &- \frac{1}{4}g_Z^2 R_{hi}R_{hj} \left(\frac{1}{\delta_{ij}+1} + 1 \right) 4m_Z^2 \\ &- (\delta_{ij}+1)\lambda_{ijG^+G^-} A(m_W) \\ &- (\delta_{ij}+1)\lambda_{ijG^0G^0} A(m_Z) \\ &+ g^2 R_{hi}R_{hj} (3m_W^2 - Q^2) B_0(Q^2, m_W, m_W) \\ &+ \frac{1}{2}g_Z^2 R_{hi}R_{hj} (3m_Z^2 - Q^2) B_0(Q^2, m_Z, m_Z) \\ &+ \lambda_{iG^+G^-} \lambda_{jG^+G^-} B_0(Q^2, m_W, m_W) \\ &+ 2\lambda_{iG^0G^0} \lambda_{jG^0G^0} B_0(Q^2, m_Z, m_Z), \end{aligned} \quad (\text{A3})$$

$$\begin{aligned} (16\pi^2)\Pi_{ij}^S &= -(c_1)_{ij} \lambda_{ij11} A(m_1) - (c_2)_{ij} \lambda_{ij22} A(m_2) \\ &+ (c_{11})_{ij} \lambda_{i11} \lambda_{j11} B_0(Q^2, m_1, m_1) \\ &+ (c_{22})_{ij} \lambda_{i22} \lambda_{j22} B_0(Q^2, m_2, m_2) \\ &+ 4\lambda_{i12} \lambda_{j12} B_0(Q^2, m_1, m_2), \end{aligned} \quad (\text{A4})$$

$$\begin{aligned} (16\pi^2)\Pi_{ij}^a &= 2\lambda_{iaa} \lambda_{jaa} B_0(Q^2, 0, 0) \\ &- (\delta_{ij}+1)\lambda_{ijaa} A(0), \end{aligned} \quad (\text{A5})$$

where N_f^c is the color factor for the fermions, $N_f^c = 3$ (1) for quarks (leptons) and the orthogonal matrix R is defined in the main text. The coefficients for c_m , c_{mn} ($m, n = 1, 2$) are defined by

$$c_1 = \begin{pmatrix} 12 & 3 \\ 3 & 2 \end{pmatrix}, \quad c_2 = \begin{pmatrix} 2 & 3 \\ 3 & 12 \end{pmatrix}, \quad (\text{A6})$$

$$c_{11} = \begin{pmatrix} 18 & 6 \\ 6 & 2 \end{pmatrix}, \quad c_{22} = \begin{pmatrix} 2 & 6 \\ 6 & 18 \end{pmatrix}. \quad (\text{A7})$$

The pinch term contributions Π_{ij}^{PT} are given by [40, 41]

$$\begin{aligned} (16\pi^2)\Pi_{ij}^{\text{PT}} &= -\frac{1}{4}R_{hi}R_{hj} (2Q^2 - m_i^2 - m_j^2) \\ &\times \{ 2g^2 B_0(Q^2, m_W, m_W) + g_Z^2 B_0(Q^2, m_Z, m_Z) \}. \end{aligned} \quad (\text{A8})$$

We also give analytical formulae for the 1-point function for ϕ_1 and ϕ_2 , which is schematically given by

$$T_i = \sum_f T_i^f + T_i^V + T_i^S + T_i^a. \quad (\text{A9})$$

Each contribution is presented by

$$(16\pi^2)T_i^f = -R_{hi} \frac{4N_f^c m_f^2}{v} A(m_f), \quad (\text{A10})$$

$$\begin{aligned} (16\pi^2)T_i^V &= \\ &+ 3R_{hi} g m_W A(m_W) + \frac{3}{2} R_{hi} g_Z m_Z A(m_Z) \\ &- 2R_{hi} \left(g m_W^3 + \frac{g_Z m_Z^3}{2} \right) \\ &- \lambda_{iG^+G^-} A(m_W) - \lambda_{iG^0G^0} A(m_Z), \end{aligned} \quad (\text{A11})$$

$$(16\pi^2)T_i^S = -\sum_{k=1}^2 (b_k)_i \lambda_{ikk} A(m_k), \quad (\text{A12})$$

$$(16\pi^2)T_i^a = -\lambda_{iaa} A(0), \quad (\text{A13})$$

where the coefficient b_m ($m = 1, 2$) satisfies

$$b_1 = (3, 1), \quad b_2 = (1, 3). \quad (\text{A14})$$

The scalar couplings are given by

$$\lambda_{1G^0G^0} = -\frac{m_1^2 \cos \alpha}{2v}, \quad (\text{A15})$$

$$\lambda_{2G^0G^0} = \frac{m_2^2 \sin \alpha}{2v}, \quad (\text{A16})$$

$$\lambda_{iG^+G^-} = 2\lambda_{iG^0G^0}, \quad (\text{A17})$$

$$\lambda_{111} = -\frac{m_1^2}{2vv_s} (v \sin^3 \alpha + v_s \cos^3 \alpha), \quad (\text{A18})$$

$$\lambda_{112} = \frac{(2m_1^2 + m_2^2)}{4vv_s} \sin(2\alpha) (v_s \cos \alpha - v \sin \alpha), \quad (\text{A19})$$

$$\lambda_{122} = -\frac{(m_1^2 + 2m_2^2)}{4vv_s} \sin(2\alpha) (v \cos \alpha + v_s \sin \alpha), \quad (\text{A20})$$

$$\lambda_{222} = -\frac{m_2^2}{2vv_s} (v \cos^3 \alpha - v_s \sin^3 \alpha), \quad (\text{A21})$$

$$\lambda_{1aa} = -\frac{m_1^2 \sin \alpha}{2v_s}, \quad (\text{A22})$$

$$\lambda_{2aa} = -\frac{m_2^2 \cos \alpha}{2v_s}, \quad (\text{A23})$$

$$\lambda_{11G^0G^0} = -\frac{\cos\alpha}{4v^2v_s} \left[(m_1^2 - m_2^2)v \sin^3\alpha \right. \\ \left. + m_1^2v_s \cos^3\alpha + m_2^2v_s \sin^2\alpha \cos\alpha \right] \quad (\text{A24})$$

$$\lambda_{12G^0G^0} = \frac{\sin\alpha \cos\alpha}{2v^2v_s} \left[(m_2^2 - m_1^2)v \sin\alpha \cos\alpha \right. \\ \left. + m_1^2v_s \cos^2\alpha + m_2^2v_s \sin^2\alpha \right] \quad (\text{A25})$$

$$\lambda_{22G^0G^0} = -\frac{\sin\alpha}{4v^2v_s} \left[(m_1^2 - m_2^2)v \cos^3\alpha \right. \\ \left. + m_1^2v_s \sin\alpha \cos^2\alpha + m_2^2v_s \sin^3\alpha \right], \quad (\text{A26})$$

$$\lambda_{ijG^+G^-} = 2\lambda_{ijG^0G^0}, \quad (\text{A27})$$

$$\lambda_{1111} = \frac{1}{8v^2v_s^2} \left[-m_1^2v^2 \sin^6\alpha - m_1^2v_s^2 \cos^6\alpha \right. \\ \left. - m_2^2v^2 \sin^4\alpha \cos^2\alpha - m_2^2v_s^2 \sin^2\alpha \cos^4\alpha \right. \\ \left. - 2(m_1^2 - m_2^2)vv_s \sin^3\alpha \cos^3\alpha \right], \quad (\text{A28})$$

$$\lambda_{1211} = -\sin(2\alpha) \frac{v \sin\alpha - v_s \cos\alpha}{16v^2v_s^2} \left[\right. \\ \left. v(3m_1^2 + m_2^2) \sin\alpha \right. \\ \left. + v(m_2^2 - m_1^2) \sin(3\alpha) \right. \\ \left. + v_s(3m_1^2 + m_2^2) \cos\alpha \right. \\ \left. + v_s(m_1^2 - m_2^2) \cos(3\alpha) \right], \quad (\text{A29})$$

$$\lambda_{2211} = -\frac{\sin\alpha \cos\alpha}{32v^2v_s^2} \left[\right. \\ \left. 6 \sin(2\alpha)(m_1^2 + m_2^2)(v^2 + v_s^2) \right. \\ \left. - (m_1^2 - m_2^2)(3(v^2 - v_s^2) \sin(4\alpha) - 2vv_s) \right. \\ \left. + 6vv_s(m_1^2 - m_2^2) \cos(4\alpha) \right], \quad (\text{A30})$$

$$\lambda_{1122} = \lambda_{2211}, \quad (\text{A31})$$

$$\lambda_{1222} = \lambda_{1211} \\ + \frac{\sin(4\alpha)}{16v^2v_s^2} \left[\cos(2\alpha)(m_1^2 - m_2^2)(v^2 - v_s^2) \right. \\ \left. - (m_1^2 + m_2^2)(v^2 + v_s^2) \right. \\ \left. + 2vv_s(m_1^2 - m_2^2) \sin(2\alpha) \right] \quad (\text{A32})$$

$$\lambda_{2222} = \lambda_{1111} \\ - \frac{\cos(2\alpha)}{8v^2v_s^2} \left[\sin^2\alpha(m_1^2v^2 - m_2^2v_s^2) \right. \\ \left. + \cos^2\alpha(m_2^2v^2 - m_1^2v_s^2) \right], \quad (\text{A33})$$

$$\lambda_{11aa} = -\frac{\sin\alpha}{4vv_s^2} \left[v_s \cos^3\alpha(m_1^2 - m_2^2) \right. \\ \left. + v \sin\alpha(\sin^2\alpha(m_1^2 - m_2^2) + m_2^2) \right], \quad (\text{A34})$$

$$\lambda_{12aa} = -\frac{\sin\alpha \cos\alpha}{2vv_s^2} \left[(m_2^2 - m_1^2)v_s \sin\alpha \cos\alpha \right. \\ \left. + m_1^2v \sin^2\alpha + m_2^2v \cos^2\alpha \right], \quad (\text{A35})$$

$$\lambda_{22aa} = -\frac{\cos\alpha}{4vv_s^2} \left[v_s(m_1^2 - m_2^2) \sin^3\alpha \right. \\ \left. + m_1^2v \sin^2\alpha \cos\alpha + m_2^2v \cos^3\alpha \right]. \quad (\text{A36})$$

Appendix B: One-loop contributions to the deviations in the Higgs boson coupling

We here evaluate the one-loop corrections to the coupling constants for the fuzzy Higgs boson h_{eff} with any SM particle X , considering the case of $|m_2^2 - m_1^2| \ll m_{\text{heff}}\Gamma_s$. The renormalized vertex function can be schematically expressed by

$$\Gamma_{\text{heff}XX} = \Gamma_{\text{heff}XX}^{\text{tree}} + \Gamma_{\text{heff}XX}^{1\text{PI}} + \delta\Gamma_{\text{heff}XX}, \quad (\text{B1})$$

where $\Gamma_{\text{heff}XX}^{\text{tree}}$ denotes the tree-level coupling $\Gamma_{\text{heff}XX}^{\text{tree}}$ and $\Gamma_{\text{heff}XX}^{1\text{PI}}$ ($\delta\Gamma_{\text{heff}XX}$) stands for contributions from the 1PI diagram (the counter term). The fuzzy Higgs boson h_{eff} can be regarded as h in the flavor basis. Hence, the tree level coupling $\Gamma_{\text{heff}XX}^{\text{tree}}$ coincides with that of the SM, i.e., $\Gamma_{\text{heff}XX}^{\text{tree}} = g_{hXX}^{\text{SM}}$, where g_{hXX}^{SM} denotes the tree level coupling in the SM, e.g., $g_{hbb}^{\text{SM}} = m_b/v$ and $g_{hWW}^{\text{SM}} = m_W/v$. The deviations from the SM prediction arise by higher-order corrections. We note that, in addition to the loop corrections to $\Gamma_{\text{heff}XX}^{\text{tree}}$, the correction to the propagator in the Higgs production $e^+e^- \rightarrow Zh_{\text{eff}}$, δ or the effective mixing α_{eff} should be also incorporated in the deviation of the Higgs couplings. It can be written by $\cos[\alpha_{\text{eff}}]g_{hXX}^{\text{SM}}$. This effect will be not included in this part, and we will see if the other loop contributions can introduce a sizable deviation.

The counter-term $\delta\Gamma_{\text{heff}XX}$ can be derived by shifting parameters and fields in the interaction term $g_{hXX}^{\text{SM}}hXX$. We perform this in the mass basis and obtain the counter terms for the $h_{\text{eff}}XX$ vertex by returning to the flavor basis with the corresponding orthogonal transformation. The shift, or kinetic normalization, of the Higgs boson fields are defined by

$$\begin{pmatrix} \phi_1 \\ \phi_2 \end{pmatrix} \rightarrow \hat{Z}^{1/2} \begin{pmatrix} \phi_1 \\ \phi_2 \end{pmatrix} \quad (\text{B2})$$

$$\text{with } \hat{Z}^{1/2} \equiv \begin{pmatrix} 1 + \frac{1}{2}\delta Z_{11} & \frac{1}{2}\delta Z_{12} \\ \frac{1}{2}\delta Z_{21} & 1 + \frac{1}{2}\delta Z_{22} \end{pmatrix}. \quad (\text{B3})$$

where δZ_{ij} ($i, j = 1, 2$) are the wave functions renormalization constants (WFRCs) for the Higgs bosons ϕ_1, ϕ_2 . Applying the shift of ϕ_1, ϕ_2 , a SM field X and the cou-

pling g_{hXX}^{SM} yield the counter term

$$\delta\Gamma_{h_{\text{eff}}XX} = g_{hXX}^{\text{SM}} \left\{ \cos^2 \alpha \frac{\delta Z_{11}}{2} + \sin^2 \alpha \frac{\delta Z_{22}}{2} - \sin \alpha \cos \alpha \left(\frac{\delta Z_{12}}{2} + \frac{\delta Z_{21}}{2} \right) \right\} + \delta\Gamma_{h_{\text{eff}}XX}^{\text{rem}}, \quad (\text{B4})$$

where $\delta\Gamma_{h_{\text{eff}}XX}^{\text{rem}}$ denotes the counter term contributions except for the Higgs bosons, which are the same as the SM at the 1-loop level. Here the first term comes from $(R\hat{Z}^{1/2}R^{-1} - \mathbf{1})_{hh} g_{hXX}^{\text{SM}}$. For completeness, we show the explicit formulae of $\delta\Gamma_{h_{\text{eff}}XX}^{\text{rem}}$ for the hbb coupling and the hWW coupling,

$$\delta\Gamma_{h_{\text{eff}}bb}^{\text{rem}} = -\frac{m_f}{v} \left(\frac{\delta m_f}{m_f} - \frac{\delta v}{v} + \frac{\delta Z_{b,L}}{2} + \frac{\delta Z_{b,R}}{2} \right), \quad (\text{B5})$$

$$\delta\Gamma_{h_{\text{eff}}WW}^{\text{rem}} = \frac{2m_W^2}{v} \left(\frac{\delta m_W^2}{m_W^2} - \frac{\delta v}{v} + \delta Z_W \right). \quad (\text{B6})$$

For the definition of counter terms of EW VEV, the masses, the WFRs for b and W , we refer, e.g., [61]. Remarkably, the counter term from the mixing angle α is canceled out in those expressions.

In actual numerical calculations for the deviations in the Higgs boson couplings, we omit $\delta\Gamma_{h_{\text{eff}}XX}^{\text{rem}}$ as well as the 1PI diagram contributions $\Gamma_{h_{\text{eff}}XX}^{\text{1PI}}$ since the s contribution does not appear in the 1-loop level.³ In Refs. [62–64] and Refs. [65, 66] one can find the calculations for the 1-loop corrections to the Higgs boson couplings in two Higgs doublet model and Higgs singlet model, respectively.

The WFRs δZ_{ij} are determined by the on-shell conditions for the Higgs bosons in the mass basis ϕ_1 and ϕ_2 [40, 41]. They are written by

$$\delta Z_{11} = -\Pi'_{11}(m_1^2), \quad \delta Z_{22} = -\Pi'_{22}(m_2^2), \quad (\text{B7})$$

$$\delta Z_{12} = -2 \frac{\tilde{\Pi}_{12}(m_2^2)}{m_2^2 - m_1^2}, \quad \delta Z_{21} = 2 \frac{\tilde{\Pi}_{12}(m_1^2)}{m_2^2 - m_1^2}, \quad (\text{B8})$$

where $\Pi'_{ii}(m_i^2) \equiv d\Pi_{ii}(Q^2)/dQ^2|_{Q^2=m_i^2}$ and $\tilde{\Pi}_{12}$ is de-

fined by

$$\tilde{\Pi}_{12} = \Pi_{12} - 2 \sin \alpha \cos \alpha \left(\frac{\delta T_h}{v} - \frac{\delta T_s}{v_s} \right) \quad (\text{B9})$$

with $\delta T_h = \cos \alpha \delta T_1 - \sin \alpha \delta T_2$ and $\delta T_s = \sin \alpha \delta T_1 + \cos \alpha \delta T_2$. For the renormalization of tadpoles, the standard tadpole scheme is used, where the counter terms for the tadpole are set in the way that the renormalized tadpoles disappear at the 1-loop level, i.e., $\hat{T}_i = T_i + \delta T_i = 0$.

We define the deviations of the Higgs boson couplings by

$$\kappa_X = \frac{\Gamma_{hXX}^{\text{heff}}}{\Gamma_{hXX}^{\text{SM}}}, \quad (\text{B10})$$

where the Γ_{hXX}^{SM} denotes the renormalized vertex function in the SM. With the obtained concrete expressions for δZ_{ij} , the deviations in the Higgs boson couplings can be written as

$$\begin{aligned} \kappa_X \sim & \left(1 - \frac{\cos^2 \alpha}{2} \Pi'_{11}(m_1^2)|_{\text{fin.}} - \frac{\sin^2 \alpha}{2} \Pi'_{22}(m_2^2)|_{\text{fin.}} \right. \\ & \left. - \frac{\sin \alpha \cos \alpha}{m_2^2 - m_1^2} \left\{ \tilde{\Pi}_{12}(m_1^2)|_{\text{fin.}} - \tilde{\Pi}_{12}(m_2^2)|_{\text{fin.}} \right\} \right) \\ & / \left(1 - \frac{1}{2} \Pi_{hh}^{\text{SM}'}(m_h^2)|_{\text{fin.}} \right), \end{aligned} \quad (\text{B11})$$

where Π_{hh}^{SM} denotes the self energy for the Higgs boson h in the SM. We take finite part of each self energy in Eq. (B11), which is denoted by $\Pi_{ij}^{(\prime)}(Q^2)|_{\text{fin.}}$. UV divergence cancels out if one involves the remaining contributions $\Gamma_{h_{\text{eff}}XX}^{\text{1PI}} + \delta\Gamma_{h_{\text{eff}}XX}$.

From numerical calculation with `LoopTools` [67], we show deviation, $\kappa_X - 1$, in Fig. 2 by varying v_s and ϵ in the upper and lower panels, respectively. We fix $\epsilon = 10 \text{ GeV}^2, 100 \text{ GeV}^2, 1000 \text{ GeV}^2$ from top to bottom in the upper panel and $v_s = 10 \text{ GeV}, 100 \text{ GeV}, 1000 \text{ GeV}$ from bottom to top in the bottom panel. The small contribution to the deviation of the Higgs coupling in the regime is due to the small portal coupling λ_P that leads to a small mass difference. This interpretation is consistent with the dependence of $|\epsilon|$. Also one can see that $|\kappa_X - 1|$ is not proportional to v_s^2 i.e. it is not suppressed by Γ_s . Thus the suppression of the deviation has a different origin from the suppression of the mixing effect in the main part. The deviations of the couplings are negligible in the regime of our interest since $|\epsilon|$ is usually not very large in the fuzzy Higgs boson scenario (at least when the dark sector is perturbative).

³ The exception is the Higgs boson self-coupling $h_{\text{eff}}h_{\text{eff}}h_{\text{eff}}$. For

this coupling, 1PI diagrams involve dominant contributions by s . This effect is also suppressed by the small $|\lambda_P|$.

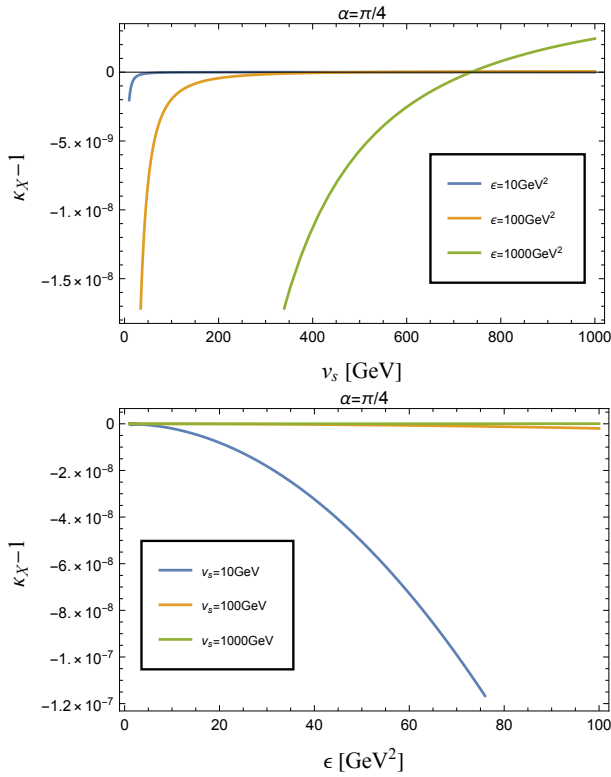


Figure 2. The deviation of the Higgs coupling, $\kappa_X - 1$ by varying v_s (upper panel) and ϵ (lower panel) with fixing $\alpha = \pi/4$.

- [1] V. Silveira and A. Zee, SCALAR PHANTOMS, *Phys. Lett. B* **161**, 136 (1985).
- [2] C. P. Burgess, M. Pospelov, and T. ter Veldhuis, The Minimal model of nonbaryonic dark matter: A Singlet scalar, *Nucl. Phys. B* **619**, 709 (2001), arXiv:hep-ph/0011335.
- [3] K. Nakayama and W. Yin, Hidden photon and axion dark matter from symmetry breaking, *JHEP* **10**, 026, arXiv:2105.14549 [hep-ph].
- [4] K. Sakurai and W. Yin, Phenomenology of CP-even ALP, (2021), arXiv:2111.03653 [hep-ph].
- [5] V. Barger, P. Langacker, M. McCaskey, M. Ramsey-Musolf, and G. Shaughnessy, Complex Singlet Extension of the Standard Model, *Phys. Rev. D* **79**, 015018 (2009), arXiv:0811.0393 [hep-ph].
- [6] V. Barger, M. McCaskey, and G. Shaughnessy, Complex Scalar Dark Matter vis-à-vis CoGeNT, DAMA/LIBRA and XENON100, *Phys. Rev. D* **82**, 035019 (2010), arXiv:1005.3328 [hep-ph].
- [7] M. Gonderinger, H. Lim, and M. J. Ramsey-Musolf, Complex Scalar Singlet Dark Matter: Vacuum Stability and Phenomenology, *Phys. Rev. D* **86**, 043511 (2012), arXiv:1202.1316 [hep-ph].
- [8] K. Ishiwata and T. Toma, Probing pseudo Nambu-Goldstone boson dark matter at loop level, *JHEP* **12**, 089, arXiv:1810.08139 [hep-ph].
- [9] J. M. Cline and T. Toma, Pseudo-Goldstone dark matter confronts cosmic ray and collider anomalies, *Phys. Rev. D* **100**, 035023 (2019), arXiv:1906.02175 [hep-ph].
- [10] B. Grzadkowski, M. Iglicki, K. Mekala, and A. F. Zarniecki, Dark-matter-spin effects at future e^+e^- colliders, *JHEP* **08**, 052, arXiv:2003.06719 [hep-ph].
- [11] Y. Abe, T. Toma, and K. Tsumura, Pseudo-Nambu-Goldstone dark matter from gauged $U(1)_{B-L}$ symmetry, *JHEP* **05**, 057, arXiv:2001.03954 [hep-ph].
- [12] S. Abe, G.-C. Cho, and K. Mawatari, Probing a degenerate-scalar scenario in a pseudoscalar dark-matter model, *Phys. Rev. D* **104**, 035023 (2021), arXiv:2101.04887 [hep-ph].
- [13] G.-C. Cho, C. Idegawa, and E. Senaha, Electroweak phase transition in a complex singlet extension of the Standard Model with degenerate scalars, *Phys. Lett. B* **823**, 136787 (2021), arXiv:2105.11830 [hep-ph].
- [14] N. Chen, T. Li, Y. Wu, and L. Bian, Complementarity of the future e^+e^- colliders and gravitational waves in the probe of complex singlet extension to the standard model, *Phys. Rev. D* **101**, 075047 (2020), arXiv:1911.05579 [hep-ph].
- [15] B. Bhattacharjee, S. Matsumoto, and R. Sengupta, Long-Lived Light Mediators from Higgs boson Decay at HL-LHC, FCC-hh and a Proposal of Dedicated LLP Detectors for FCC-hh, (2021), arXiv:2111.02437 [hep-ph].
- [16] S. Weinberg, *The quantum theory of fields*, Vol. 2 (Cambridge university press, 1995).
- [17] H. Nakazato, M. Namiki, and S. Pascazio, Temporal behavior of quantum mechanical systems, *Int. J. Mod. Phys. B* **10**, 247 (1996), arXiv:quant-ph/9509016.
- [18] E. K. Akhmedov, V. A. Rubakov, and A. Y. Smirnov, Baryogenesis via neutrino oscillations, *Phys. Rev. Lett.* **81**, 1359 (1998), arXiv:hep-ph/9803255.
- [19] T. Asaka and M. Shaposhnikov, The ν MSM, dark matter and baryon asymmetry of the universe, *Phys. Lett. B* **620**, 17 (2005), arXiv:hep-ph/0505013.
- [20] L. Canetti, M. Drewes, T. Frossard, and M. Shaposhnikov, Dark Matter, Baryogenesis and Neutrino Oscillations from Right Handed Neutrinos, *Phys. Rev. D* **87**, 093006 (2013), arXiv:1208.4607 [hep-ph].
- [21] Y. Hamada and R. Kitano, Primordial Lepton Oscillations and Baryogenesis, *JHEP* **11**, 010, arXiv:1609.05028 [hep-ph].
- [22] Y. Hamada, R. Kitano, and W. Yin, Leptogenesis via Neutrino Oscillation Magic, *JHEP* **10**, 178, arXiv:1807.06582 [hep-ph].
- [23] S. Eijima, R. Kitano, and W. Yin, Throwing away anti-matter via neutrino oscillations during the reheating era, *JCAP* **03**, 048, arXiv:1908.11864 [hep-ph].
- [24] T. Asaka, H. Ishida, and W. Yin, Direct baryogenesis in the broken phase, *JHEP* **07**, 174, arXiv:1912.08797 [hep-ph].
- [25] D. McKeen and A. E. Nelson, CP Violating Baryon Oscillations, *Phys. Rev. D* **94**, 076002 (2016), arXiv:1512.05359 [hep-ph].
- [26] K. Aitken, D. McKeen, T. Neder, and A. E. Nelson, Baryogenesis from Oscillations of Charmed or Beautiful Baryons, *Phys. Rev. D* **96**, 075009 (2017), arXiv:1708.01259 [hep-ph].
- [27] G. Elor, M. Escudero, and A. Nelson, Baryogenesis and Dark Matter from B Mesons, *Phys. Rev. D* **99**, 035031 (2019), arXiv:1810.00880 [hep-ph].
- [28] F. Chadha-Day, Axion-like particle oscillations, *JCAP* **01** (01), 013, arXiv:2107.12813 [hep-ph].
- [29] G. Cacciapaglia, A. Deandrea, and S. De Curtis, Nearby

- resonances beyond the Breit-Wigner approximation, Phys. Lett. B **682**, 43 (2009), arXiv:0906.3417 [hep-ph].
- [30] N. Arkani-Hamed, J. L. Feng, L. J. Hall, and H.-C. Cheng, CP violation from slepton oscillations at the LHC and NLC, Nucl. Phys. B **505**, 3 (1997), arXiv:hep-ph/9704205.
- [31] A. Pilaftsis, Resonant CP violation induced by particle mixing in transition amplitudes, Nucl. Phys. B **504**, 61 (1997), arXiv:hep-ph/9702393.
- [32] E. Fuchs, S. Thewes, and G. Weiglein, Interference effects in BSM processes with a generalised narrow-width approximation, Eur. Phys. J. C **75**, 254 (2015), arXiv:1411.4652 [hep-ph].
- [33] E. Fuchs and G. Weiglein, Breit-Wigner approximation for propagators of mixed unstable states, JHEP **09**, 079, arXiv:1610.06193 [hep-ph].
- [34] L. Bian, N. Chen, and Y. Zhang, CP violation effects in the diphoton spectrum of heavy scalars, Phys. Rev. D **96**, 095008 (2017), arXiv:1706.09425 [hep-ph].
- [35] B. Das, S. Moretti, S. Munir, and P. Poulou, Two Higgs bosons near 125 GeV in the NMSSM: beyond the narrow width approximation, Eur. Phys. J. C **77**, 544 (2017), arXiv:1704.02941 [hep-ph].
- [36] B. Das, S. Moretti, S. Munir, and P. Poulou, Quantum interference among heavy NMSSM Higgs bosons, Phys. Rev. D **98**, 055020 (2018), arXiv:1804.10393 [hep-ph].
- [37] B. Das, S. Moretti, S. Munir, and P. Poulou, Quantum interference effects in Higgs boson pair-production beyond the Standard Model, Eur. Phys. J. C **81**, 347 (2021), arXiv:2012.09587 [hep-ph].
- [38] S. M. Moosavi Nejad, S. Abbaspour, and R. Farashahian, Interference effects for the top quark decays $t \rightarrow b + W^+ / H^+ (\rightarrow \tau^+ \nu_\tau)$, Phys. Rev. D **99**, 095012 (2019), arXiv:1904.09680 [hep-ph].
- [39] V. Khachatryan et al. (CMS), Observation of the Diphoton Decay of the Higgs Boson and Measurement of Its Properties, Eur. Phys. J. C **74**, 3076 (2014), arXiv:1407.0558 [hep-ex].
- [40] M. Krause, R. Lorenz, M. Muhlleitner, R. Santos, and H. Ziesche, Gauge-independent Renormalization of the 2-Higgs-Doublet Model, JHEP **09**, 143, arXiv:1605.04853 [hep-ph].
- [41] S. Kanemura, M. Kikuchi, K. Sakurai, and K. Yagyu, Gauge invariant one-loop corrections to Higgs boson couplings in non-minimal Higgs models, Phys. Rev. D **96**, 035014 (2017), arXiv:1705.05399 [hep-ph].
- [42] Combination of searches for invisible Higgs boson decays with the ATLAS experiment, (2020).
- [43] M. Aaboud et al. (ATLAS), Combination of searches for invisible Higgs boson decays with the ATLAS experiment, Phys. Rev. Lett. **122**, 231801 (2019), arXiv:1904.05105 [hep-ex].
- [44] A. M. Sirunyan et al. (CMS), Search for invisible decays of a Higgs boson produced through vector boson fusion in proton-proton collisions at $\sqrt{s} = 13$ TeV, Phys. Lett. B **793**, 520 (2019), arXiv:1809.05937 [hep-ex].
- [45] G. Aad et al. (ATLAS), Combined measurements of Higgs boson production and decay using up to 80 fb⁻¹ of proton-proton collision data at $\sqrt{s} = 13$ TeV collected with the ATLAS experiment, Phys. Rev. D **101**, 012002 (2020), arXiv:1909.02845 [hep-ex].
- [46] Combined Higgs boson production and decay measurements with up to 137 fb⁻¹ of proton-proton collision data at $\sqrt{s} = 13$ TeV, (2020).
- [47] D. M. Asner et al., ILC Higgs White Paper, in Community Summer Study 2013: Snowmass on the Mississippi (2013) arXiv:1310.0763 [hep-ph].
- [48] D. d'Enterria, Physics at the FCC-ee, in 17th Lomonosov Conference on Elementary Particle Physics (2017) pp. 182–191, arXiv:1602.05043 [hep-ex].
- [49] H. Abramowicz et al., Higgs physics at the CLIC electron-positron linear collider, Eur. Phys. J. C **77**, 475 (2017), arXiv:1608.07538 [hep-ex].
- [50] M. Ahmad et al., CEPC-SPPC Preliminary Conceptual Design Report. 1. Physics and Detector, (2015).
- [51] A. Hektor, A. Hryczuk, and K. Kannike, Improved bounds on \mathbb{Z}_3 singlet dark matter, JHEP **03**, 204, arXiv:1901.08074 [hep-ph].
- [52] R. Daido, F. Takahashi, and W. Yin, The ALP miracle: unified inflaton and dark matter, JCAP **05**, 044, arXiv:1702.03284 [hep-ph].
- [53] F. Carta, N. Righi, Y. Welling, and A. Westphal, Harmonic hybrid inflation, JHEP **12**, 161, arXiv:2007.04322 [hep-th].
- [54] R. Daido, F. Takahashi, and W. Yin, The ALP miracle revisited, JHEP **02**, 104, arXiv:1710.11107 [hep-ph].
- [55] E. Armengaud et al. (IAXO), Physics potential of the International Axion Observatory (IAXO), JCAP **06**, 047, arXiv:1904.09155 [hep-ph].
- [56] S.-M. Choi, Y.-J. Kang, H. M. Lee, and K. Yamashita, Unitary inflaton as decaying dark matter, JHEP **05**, 060, arXiv:1902.03781 [hep-ph].
- [57] F. Takahashi and W. Yin, ALP inflation and Big Bang on Earth, JHEP **07**, 095, arXiv:1903.00462 [hep-ph].
- [58] F. Takahashi, M. Yamada, and W. Yin, What if ALP dark matter for the XENON1T excess is the inflaton, JHEP **01**, 152, arXiv:2007.10311 [hep-ph].
- [59] F. Takahashi and W. Yin, Challenges for heavy QCD axion inflation, JCAP **10**, 057, arXiv:2105.10493 [hep-ph].
- [60] G. Passarino and M. J. G. Veltman, One Loop Corrections for $e^+ e^-$ Annihilation Into $\mu^+ \mu^-$ in the Weinberg Model, Nucl. Phys. B **160**, 151 (1979).
- [61] A. Denner, Techniques for calculation of electroweak radiative corrections at the one loop level and results for W physics at LEP-200, Fortsch. Phys. **41**, 307 (1993), arXiv:0709.1075 [hep-ph].
- [62] S. Kanemura, Y. Okada, E. Senaha, and C. P. Yuan, Higgs coupling constants as a probe of new physics, Phys. Rev. D **70**, 115002 (2004), arXiv:hep-ph/0408364.
- [63] S. Kanemura, M. Kikuchi, and K. Yagyu, Radiative corrections to the Yukawa coupling constants in two Higgs doublet models, Phys. Lett. B **731**, 27 (2014), arXiv:1401.0515 [hep-ph].
- [64] S. Kanemura, M. Kikuchi, and K. Yagyu, Fingerprinting the extended Higgs sector using one-loop corrected Higgs boson couplings and future precision measurements, Nucl. Phys. B **896**, 80 (2015), arXiv:1502.07716 [hep-ph].
- [65] S. Kanemura, M. Kikuchi, and K. Yagyu, Radiative corrections to the Higgs boson couplings in the model with an additional real singlet scalar field, Nucl. Phys. B **907**, 286 (2016), arXiv:1511.06211 [hep-ph].
- [66] S. Kanemura, M. Kikuchi, and K. Yagyu, One-loop corrections to the Higgs self-couplings in the singlet extension, Nucl. Phys. B **917**, 154 (2017), arXiv:1608.01582 [hep-ph].
- [67] T. Hahn and M. Perez-Victoria, Automatized one

loop calculations in four-dimensions and D-dimensions,

Comput. Phys. Commun. **118**, 153 (1999), arXiv:hep-ph/9807565.